Composite Structures

Volume 141, 1 May 2016, Pages 146–154

doi:10.1016/j.compstruct.2016.01.031

http://www.sciencedirect.com/science/article/pii/S0263822316000441

FRACTURE RESISTANCE OF HYBRID PP/ELASTOMER/WOOD COMPOSITES

A. Sudár[1,2], K. Renner[1,2*], J. Móczó[1,2], T. Lummerstorfer[3], Ch. Burgstaller[4], M. Jerabek[3], M. Gahleitner[3], P. Doshev[3], and B. Pukánszky[1,2]

[1]Laboratory of Plastics and Rubber Technology, Department of Physical Chemistry and Materials Science, Budapest University of Technology and Economics, H-1521 Budapest, P.O. Box 91, Hungary

[2]Institute of Materials and Environmental Chemistry, Chemical Research Center, Hungarian Academy of Sciences, H-1519 Budapest, P.O. Box 286, Hungary

[3]Borealis Polyolefine GmbH, St.-Peter-Strasse 25, A-4021 Linz, Austria

[4]Transfercenter für Kunststofftechnik GmbH, Franz-Fritsch-Strasse 11, A-4600 Wels, Austria

*Corresponding author: Phone: +36-1-463-2479, Fax: +36-1-463-3474, Email: krenner@mail.bme.hu

ABSTRACT

PP was modified with elastomer and wood to prepare materials with large stiffness and impact resistance. Three wood fibers with different particle characteristics were used, and elastomer as well as wood content changed in a wide range. Interfacial adhesion was modified through the use of maelated polypropylene (MAPP) coupling agent. The structure of ternary PP/elastomer/wood composites was manipulated by the use of functionalized polymers and processing conditions. Considerable embedding of the wood into the elastomer was achieved in some cases depending on the variables. Wood increases impact resistance slightly, elastomer drastically in two-component composites and blends, but fracture toughness remains small in three-component hybrid systems irrespectively of structure. Depending on particle size and interfacial adhesion fiber fracture and debonding occur in wood reinforced composites, mainly plastic deformation takes place in blends. This latter process is suppressed by cavitation promoted further by the presence of wood fibers which increase local stresses. The usual concept of three-component materials does not work in wood composites, micromechanical deformations must be controlled to diminish or completely eliminate cavitation

and to increase the plastic deformation of the matrix polymer.

KEYWORDS: PP/elastomer/wood composites, impact modification, interfacial adhesion, composite structure, deformation mechanism

1. Introduction

The building [1] as well as the automotive [2] industry use a large amount of structural materials made from plastics. In structural applications often large stiffness and impact resistance are required simultaneously. Polypropylene (PP) has reasonable stiffness, but poor impact resistance especially at low temperatures. Stiffness can be increased further by the application of fillers or fibers, but such a modification decreases fracture resistance even more. On the other hand, impact strength is usually increased by elastomer modification that can be done in the reactor or by blending [3]. Unfortunately the presence of elastomers decreases stiffness considerably. As a consequence, the simultaneous increase of stiffness and impact resistance is often achieved by the combination of the two additives. Bumper materials represent a typical example containing an elastomer and a filler or fiber [4-6]. In this application, the most often used fillers or reinforcements are talc [7] and glass fibers, while mainly ethylene-propylene (EPR) or ethylene-propylene-diene (EPDM) copolymers are applied as elastomers. Research has started as

early as the 80ies on these materials [6, 8-12] and they are commercially available for several decades.

Two boundary structures may form in such three-component materials: the two components, i.e. the elastomer and the filler, may be distributed separately from each other in the polymer matrix [13-15], or the elastomer may encapsulate the reinforcement to create embedded structure [4-6, 16]. The actual structure is determined by the adhesion and shear forces prevailing in the melt during homogenization, the first favoring embedding because of thermodynamic reasons, while the second resulting in separate dispersion through the shearing apart of the layered structure [17]. Usually intermediate structures form in composites produced under practical conditions, a part of the filler is embedded into the elastomer phase, but individual elastomer droplets and filler particles can be also located in the matrix. Structure can be tailored by controlling interfacial adhesion through the use of appropriate coupling agents [17-20]. The addition of maleated PP (MAPP) leads almost exclusively to separate dispersion, while that of maleated ethylene-propylene-diene elastomer (MAEPDM), results in a large extent of embedding. Properties change considerably with structure even at the same composition. Stiffness was shown to depend mainly on the extent of embedding, but impact resistance was influenced also by other factors including local deformation processes

occurring around the inclusions (elastomer, filler) [21].

It seems to be obvious to use wood and/or natural fibers to replace mineral fillers or glass fibers also in such composites. Wood flour and natural fibers are used in increasing quantities for the reinforcement of commodity polymers including PP [22-24]. Such reinforcements have many advantages over particulate fillers or glass fibers; they increase stiffness considerably, they are obtained from renewable resources, available in abundant quantities, cheap, and light at the same time [2,4,5,23,25,26]. However, wood flour differs considerably from traditional reinforcements. Wood particles are large, usually several 100 μm in size that facilitates debonding, the separation of the matrix/filler interface already at small stresses [27-29]. A functionalized polymer coupling agent is needed practically always in order to achieve reasonable properties, at least in polyolefin composites [30-34]. At strong interfacial adhesion, large wood particles may also initiate other local deformation processes during the deformation of the composite like fiber pull-out, or fiber fracture [27, 28]. Although the differences between particulate fillers and wood fibers require a more detailed study of the behavior of multicomponent materials containing wood fibers, very few papers have been published in this area yet. A model study was carried out on the recycling of PP/PE blends by Clemons [35], and functionalized elastomers were

used to modify structure and properties in PP/wood composites by Oksman [36, 37].

In a previous study [38] we investigated the effect of component properties, composition and interfacial adhesion on the fracture resistance of PP/elastomer/wood composites. We used a PP homopolymer as matrix, a wood flour with large particle size as reinforcement and two functionalized polymers, an MAPP and an MAEPDM to control structure. Unfortunately, the combination of the selected components and processing conditions resulted in the separate distribution of the components practically always thus the effect of structure could not be studied basically at all. As a consequence, we selected different components in this work and varied the properties of the additives, including that of the wood, the coupling agent (MAPP) and the elastomer, in order to change structure in a wider range. The goal of the study was to determine the effect of composition and structure on the impact resistance of three-component hybrid PP materials, identify deformation and failure mechanisms and create guidelines for the development of structural materials with large stiffness and impact strength.

2. Experimental

A PP homopolymer (hPP, Daplen HJ 325 MO, MFR = 50 g/10 min at 230 °C and 2.16 kg load) and a reactor blend (ePP, Daplen EE 050, MFR = 50 g/10 min at 230 °C and 2.16 kg load)

were used as matrix polymers used in the study. Both were supplied by Borealis AG, Austria. In order to study the effect of elastomer content the Dutral CO 038 PL ethylene-propylene copolymer with an ethylene content of 72 wt% and a Mooney viscosity, ML (1+4) of 60 measured at 125 °C from Polimeri Europa, Italy was added to the reactor blend. To obtain copolymers with smaller elastomer content than 33 wt%, the reactor blend was diluted with the HJ 325 MO homopolymer. Two maleated PP polymers were applied to achieve the separate distribution of the components; they differed in MFR in order to change shear stresses during homogenization and further control structure. The Scona 2112 grade had an MFR of 2.7 g/10 min at 190 °C and 2.16 kg load and a maleic anhydride (MAH) content of 0.9-1.2 %), while the Scona 8112 polymer had and MFR of 80 g/10 min MFR measured under the same conditions and a MAH content of 1.4 %. Both polymers were supplied by BYK Chemie GmbH, Switzerland. Maleated EPDM was used to promote embedding. The Exxcellor VA 1803 grade with an ethylene content of 43 wt% and an MFR value of 22 g/10 min (230 °C and 2.16 kg) was applied in the study. Its MA content was 0.5-1.0 wt% (Exxon Mobil, USA). Three wood flour grades were used as reinforcement, all three supplied by Rettenmaier and Söhne GmbH, Germany. The average particle size of the fillers changed between 10 and 160 μm and their aspect ratio also varied somewhat. The particle characteristics of the wood

fillers are compiled in **Table 1**. MAPP was always added in 10 wt% calculated for the amount of wood [39], while the elastomers (EPR, MAEPR) were introduced in 0, 20, 33 and 43 wt% of the matrix polymer. Wood content changed from 0 to 40 wt% in 7 steps related to the total weight of the composites.

The composites were homogenized using a ThermoPrism TSE 24 (Thermo Fisher Sci. Inc., Waltham, USA) twin-screw extruder with a screw diameter of 24 mm and an L/D ratio of 28. Screw configuration included two kneading zones with different lengths and conveying elements. The polymer components were introduced into the hopper, while wood was added to the melt through a side feeder. Zone temperatures were changed from 170 to 220 °C in 10 °C steps in the six zones of the extruder. The granulated material was dried for 4 hours at 105 °C in an oven and then injection molded to standard ISO 527 1A tensile specimens using a Demag IntElect 50 machine (Demag Ergotech GmbH, Schwaig, Germany) at 170-180-190-200-210 °C zone and 50 °C mold temperatures, 50 mm/s injection rate, max. 1300 bar holding pressure and 25 s holding time. The samples were conditioned at 23 °C and 50 % RH for a week before testing.

The extent of embedding was deduced from the composition dependence of Young's modulus. Tensile testing was carried out using an Instron 5566 type machine (Instron Co., Canton, USA). Stiffness was determined at 0.5 mm/min. A variety of impact tests were carried out in the study. Notched Charpy impact

resistance was determined according to the ISO 179 standard at 23 and -20 °C with 2 mm notch depth. Un-notched impact was measured at room temperature (23 °C, 50 % RH). Instrumented impact testing was carried out using a Ceast Resil 5.5 instrument (CEAST spa, Pianezza, Italy) with a 4 J hammer. The structure of the composites was studied also by scanning electron microscopy using a Jeol JSM 6380 LA apparatus (JEOL Ltd., Tokyo, Japan). The distribution of the components in the matrix was determined on fracture surfaces created at liquid nitrogen temperature. Samples containing elastomer were etched in n-hexane for 1 min. SEM micrographs were recorded also on surfaces created in the impact test in order to determine the mechanism of failure. Etching was used when appropriate.

3. Results and discussion

The results are discussed in several sections. We refrain from the presentation of all of them, because of their very large number. We focus on the most important questions instead, on the effect of the variables on impact resistance. In the first two sections we show the influence of wood particles and elastomer on the impact resistance of two-component composites and blends. The fracture of three-component hybrid materials is presented next and then general correlations as well practical consequences are discussed in the last section.

3.1. PP/wood composites

Wood is expected to decrease the impact resistance of PP. However, a considerable number of examples exist which show a maximum in fracture resistance as the amount of filler increases in the composite [40-47]. The main reason for the maximum is that the dominating deformation mechanism is debonding in a large number of composites containing particulate fillers, and debonding requires energy, on the one hand, while it facilitates the deformation of the matrix, on the other. The number of possible local deformation processes is larger in composites containing wood than in those prepared with particulate fillers. As a consequence, first we investigated the effect of the three wood flours on the impact resistance of hPP composites.

Notched Charpy impact strength is plotted against wood content in **Fig. 1** for the three sets of composites. Additionally, the effect of interfacial adhesion is also shown in the figure. Although the standard deviation of the data is quite large the effect of the two variables, particle size and adhesion is very clear. Impact strength increases slightly with wood content for the composites containing the large particles, while remains approximately constant or decreases continuously for those prepared with the filler of the smaller particle sizes. Either debonding or the fracture of the wood

particles must result in the increase in the first case. The debonding of large particles is easier, thus more debonding might take place in composites containing the W160 particles than in those with the W10 filler. As mentioned above both debonding and the subsequent local deformation of the matrix consumes energy. The fracture of the particles may also explain the increase. More energy is needed for the fracture of larger particles, in fact the very small ones may not fracture at all. The considerable fracture strength of glass fiber reinforced composites results from the fracture of the fibers and fiber fracture was proved to be the dominating local deformation process in wood composites with good adhesion, in the presence of MAPP [27-29, 48]. Only further evidence may decide the reason for increasing impact strength in the case of the larger particles and for its decrease for the smaller ones.

Stiffness does not depend very much on interfacial adhesion [49], but very large differences were shown in tensile strength in the presence and absence of an efficient coupling agent. The strength of PP/wood composites containing a functionalized PP (MAPP) coupling agent is considerably larger than without coupling, in the case of poor adhesion. Quite surprisingly, adhesion has only a very slight effect on impact resistance in the PP composites studied. Impact strength seems to be slightly smaller at good adhesion, but

the effect is very small indeed. Debonding and the subsequent local deformation might play a role and good adhesion hinders these processes. However, we can conclude from this slight effect that the increase of impact strength with increasing particle size is mainly caused by the fracture of the particles and not by debonding.

Instrumented impact testing may offer further information about the fracture process which can be divided into two parts, fracture initiation and crack propagation. Force vs. time traces are presented in **Fig. 2** for the composite containing various amounts of the W160 wood flour and a MAPP coupling agent. The critical force, i.e. stress intensity factor, at which fracture is initiated increases somewhat with wood content, but otherwise the traces are very similar to each other, the specimens fail with instable crack propagation and the energy consumed is very small. Obviously, increasing stiffness and good adhesion hinders crack initiation, but propagation remains extremely fast. The quantitative analysis of maximum strength (F_{max}) and the area under the traces, i.e. fracture energy, confirms the conclusions drawn by the direct observation of the traces, but does not supply additional information.

The composition dependence of the impact resistance of the composites measured on un-notched specimens is completely different from that presented in **Fig. 1**. As **Fig. 3** shows impact

strength is much larger in this case, around 15 kJ/m^2 even at the largest wood content compared to the value of around 2 kJ/m^2 obtained in the case of the notched specimens, but it decreases continuously with increasing wood content. Crack initiation must consume more energy in the un-notched specimens; one can only speculate about crack propagation energy. Larger particles seem to be less advantageous in this case that can be explained by the larger probability of having flaws which initiate the crack. Instrumented impact testing completely confirms this tentative explanation (**Fig. 4**). F_{max} is much larger, around 500 N, than for the notched specimens and does not change with composition. On the other hand, the area under the traces, i.e. fracture energy is very small even at the smallest wood content and it remains more or less constant, or decreases slightly with increasing wood content. These results clearly prove that local processes occurring around or in the wood particles determine both crack initiation and propagation and finally the impact strength of the material.

We supported the fracture measurements with a SEM study to identify the dominating local processes, if possible. **Fig. 5** shows the fracture surface of hPP/wood composites created during the impact test. The fracture of large wood particles can be seen in **Fig. 5a**; other micrographs confirmed that particle fracture is the dominating process in the composites

containing the large particles (W160) and a coupling agent. The fracture surface recorded on the composite containing the smallest wood (**Fig. 5b**), on the other hand, is completely different. Fiber fracture cannot be seen in the micrograph practically at all, mainly a few debonded particles are visible. We may conclude from the SEM study that the increase in fracture strength observed in **Fig. 1** is caused mainly by the fracture of large wood particles, while debonding results in only small energy consumption as shown by the behavior of composites containing the small particles, which do not break, as well as by the small effect of interfacial adhesion. Nevertheless, we may say that the fracture of wood is beneficial and increases slightly the impact resistance of hPP/wood composites.

3.2. PP/elastomer blends

Elastomers are routinely used for the impact modification of brittle polymers since many years [50-53]. They initiate or promote local deformation processes, like shear yielding or crazing, which consume considerable energy. As a consequence, we do not elaborate on the topic, but show the effect of elastomers in our materials. Impact resistance is plotted against elastomer content in **Fig. 6**. At 40 wt% elastomer content we reach a notched Charpy impact resistance of about 60 kJ/m^2 compared to the 2.5 kJ/m^2 measured in hPP

wood composites. In PP, elastomers facilitate shear yielding resulting in large energy consumption. Instrumented impact traces give additional information about the fracture process. The incorporation of the elastomer increases both fracture initiation stress and crack propagation energy. However, while F_{max} values are in the same range as in hPP/wood composites, crack propagation energies are larger of about an order of magnitude. Moreover, the comparison of the traces shows that although at 20 wt% elastomer content the propagation of the crack is instable leading to catastrophic failure, at larger elastomer contents constant input of energy is needed to propagate the crack and break the specimen. The quantitative analysis of the traces clearly showed that fracture is completely dominated by crack propagation, the composition dependence of impact resistance and crack propagation energy is identical. We can conclude that the elastomer used in this study increases impact resistance very efficiently.

3.3. Hybrid composites

The results presented in the previous two paragraphs showed that wood particles may increase impact resistance slightly, while the addition of elastomer improves it considerably. As a consequence, one would expect that the impact resistance of hybrid composites also increases in an extent depending on composition and structure. Wood increases

stiffness at the same time, thus the targeted simultaneous increase of stiffness and impact resistance might be achieved. Naturally, properties depend on structure, thus the occurrence and extent of embedding must be known in order to properly evaluate the effect of structure on impact strength.

Model calculations proved that thermodynamics favors the formation of embedded structure [16]. On the other hand, weak interfacial adhesion and large shear destroys the embedded structure formed, separate the layers [16]. Besides being an important characteristic of structural materials, the stiffness of PP composites containing an elastomer and a reinforcement at the same time offers valuable information also about structure. The elastomer decreases stiffness, but otherwise the effect of the components is additive in the case of separate dispersion. On the other hand, embedding results in an additional decrease of stiffness, the extent of which can be used for the estimation of the amount of embedded particles [21]. The composition dependence of Young's modulus is plotted against wood content in **Fig. 8** for the three wood fibers in the presence of either MAPP or MAEPDM functionalized polymer. In the case of large particles and good adhesion, modulus increases steeply with increasing wood content, as expected. Obviously, the presence of MAPP favors the separate distribution of the components. On the other hand, stiffness decreases with increasing wood content when the composites

contain the small particles (W10) and MAEPR, i.e. considerable embedding takes place in this case. The figure clearly shows that structure changes in a wide range from very small to very large extent of embedding. As a consequence, similarly large differences are expected in impact resistance.

The impact strength of the same composites as in **Fig. 8** is plotted against wood content in **Fig. 9**. Quite surprisingly all the points fall onto the same correlation, structure does not seem to influence impact resistance at all. Slight differences may be discovered at the two smallest wood contents; decreasing particle size and separate distribution of the components seem to lead to better fracture resistance. However, considering the large changes in stiffness indicating significantly differing structures, the result shown in **Fig. 9** is extremely surprising. The lack of any effect from particle size might be accepted easily, since it was small anyway (see **Fig. 1**), but the complete lack of improvement in impact strength upon the addition of the elastomer is really unexpected. Apparently the factor which dominates impact resistance is wood content and all the rest is ineffective.

As before, instrumented impact testing may give further information about the fracture process and the reason for the small impact resistance. Force vs. time traces are presented in **Fig. 10** for composites containing 43 wt% elastomer, different amounts of the largest wood particles and MAPP,

since **Fig. 9** indicated larger fracture resistance in the case of separate distribution. The traces clearly show that although wood increases F_{max}, i.e. hinders crack initiation, crack propagation becomes very fast with increasing wood content and fracture energy decreases as a result. For one reason or other, the combination of wood and elastomer results in easier crack propagation.

SEM study of fracture surfaces presented the usual features. As **Fig. 11a** shows, large particles break along their axis, the dominating local deformation process is the fracture of the particles. On the other hand, mainly debonding takes place in composites containing the smallest particles as shown by **Fig. 11b**. The elastomer is not visible in the micrographs, processes related to wood particles determine properties including fracture resistance. However, a closer scrutiny of certain micrographs shows the presence a large number of small holes on the fracture surface of the composites (**Fig. 11c**). We must emphasize here that the surface was not etched, the voids formed in the fracture process. Since the size of the holes more or less corresponds to that of the elastomer, we may assume that beside the fracture of wood particles, an additional, elastomer related process also occurs in the hybrid composites. The study of numerous micrographs showed that the number of visible cavities increases both with elastomer and wood content. The process cannot be favorable

for impact resistance, since impact strength did not increase, but decreased with wood content irrespectively of structure or elastomer content.

3.4. Discussion

The results presented in previous sections indicated that both wood and the elastomer increased impact resistance, however, impact strength was very small in the hybrid composites. Wood related processes remained the same as in two-component PP/wood composites, but a new process, possibly cavitation, appeared in elastomer modified blends and in the three-component composites. Since the goal of using hybrid materials is the simultaneous increase of stiffness and impact resistance, the two quantities are often plotted against each other. **Fig. 12** presents the results in this form. A very close correlation is obtained with practically no deviating points; the correlation corresponds to the general tendency observed in all heterogeneous structural materials. In the case of the simultaneous increase of the two quantities points should have moved towards the upper right corner of the graph. The figure clearly shows that no new energy adsorption process is created in the hybrid composite and local deformations usually facilitated by the elastomer is suppressed by wood.

The elastomer forms a heterogeneous phase in the PP/elastomer blends and in the hybrid composites. The dominating local deformation process should be shear yielding,

but the appearance of the holes indicates otherwise. Cavitation is accompanied by volume increase during deformation, while shear yielding is not. The volume strain of the two matrix materials used, i.e. the homopolymer and the reactor blend, is plotted against longitudinal deformation in **Fig. 13**. The corresponding stress vs. deformation traces are also included for reference. The figure clearly shows that volume increase is significantly larger in the reactor blend than in the homopolymer proving that the holes observed in **Fig. 11c** are formed by cavitation indeed, elastomer particles break within themselves during deformation. Blends were prepared with various amounts of elastomer both from the homopolymer and the reactor blend. Their impact strength is plotted in **Fig. 14** against elastomer content. The increase in impact resistance is significantly larger in the melt blend than in the reactor blend, the mechanism of deformation must be dissimilar. SEM micrographs recorded on the fracture surface of the two kinds of blends showed significant plastic deformation in the former (**Fig. 15a**) and no plastic deformation, but exclusive cavitation in the second (**Fig. 15b**). Apart from wood related processes occurring during fracture, the dominating local deformation process in composites based on the reactor blend is cavitation which does not absorb much energy.

A large number of factors were changed in this study. The

characteristics of the wood (size, aspect ratio), the properties of the functionalized polymer (MFR), elastomer content, interfacial adhesion, structure and wood content were changed in a relatively wide range. None of them except wood content influenced impact resistance, the increased fracture resistance expected from the elastomer was not achieved. As mentioned earlier, elastomers usually facilitate the local plastic deformation of the matrix, but that did not happen in our case. Although crack initiation was hindered slightly by wood particles at good adhesion, crack propagation was facilitated by them and energy consumption decreased. All evidence shows that the crack propagates easily through large particles and debonding occurs in the case of small ones in spite of the presence of a functionalized polymer improving adhesion. This latter process does not result in the plastic deformation of the matrix, because wood increases stiffness and decreases local deformation. The elastomer cannot help either, because instead of facilitating the deformation of the matrix, cavitation occurs within the particles which does not consume much energy. Cavitation becomes more intense with increasing wood content because of increasing stiffness result in larger local stresses around them and easier cavitation. Accordingly the amount of wood dominates fracture for several reasons: the fracture of wood particles, increased stiffness and cavitation all facilitate crack propagation and decrease

fracture energy. New deformation mechanism must be initiated or the plastic deformation of the matrix must be increased in order to achieve larger impact strength in these hybrid composites.

4. Conclusions

PP/wood composites are advantageous in many respects, but their impact resistance does not meet requirements. The structure of ternary PP/elastomer/wood composites can be manipulated by the use of functionalized polymers and processing conditions and the extent of embedding changed in a wide range in our composites. Wood increases impact resistance slightly, elastomer drastically in two-component materials, but fracture toughness remains small in three-component hybrid systems irrespectively of structure. Depending on particle size and interfacial adhesion, fiber fracture and debonding occur in wood reinforced composites, while mainly plastic deformation takes place in blends. This latter process is suppressed by cavitation promoted further by the presence of wood fibers, which increase local stresses. The usual concept of three-component materials does not work in wood composites, micromechanical deformations must be controlled to diminish or completely eliminate cavitation and to increase the plastic deformation of the matrix polymer.

5. Acknowledgements

The significant help of Zoltán Link and Szabolcs Kalmár in sample preparation and impact testing is highly appreciated by the authors. We thank Hermann Braun for his help in the management and logistics of the project as well as Borealis, TVK and Clariant for the donation of materials. The authors acknowledge the financial support of Borealis and the National Scientific Research Fund of Hungary (OTKA Grant No K 101124 and PD 112489) for this project on the structure-property correlations of polymeric materials. One of the authors (Károly Renner) expresses his gratitude to the János Bolyai Research Scholarship of the Hungarian Academy of Sciences for its financial support.

6. References

[1] Güneri A. Polymers in Construction. Shrewsbury: Rapra Technology Limited; 2005.

[2] Elliott ANA. Automotive applications of polymers II. Shrewsbury: Rapra Technology Limited; 1992.

[3] Gahleitner M, Tranninger C, Doshev P. Heterophasic copolymers of polypropylene: Development, design principles, and future challenges. J Appl Polym Sci 2013;130(5):3028-3037.

[4] Stamhuis JE. Mechanical-properties and morphology of polypropylene composites. 2. Effect of polar components

in talc-filled polypropylene. Polym Compos 1988;9(1):72-77.

[5] Stamhuis JE. Mechanical-properties and morphology of polypropylene composites. 3. Short glass-fiber reinforced elastomer modified polypropylene. Polym Compos 1988;9(4):280-284.

[6] Stamhuis JE. Mechanical-properties and morphology of polypropylene composites. Talc-filled, elastomer-modified polypropylene. Polym Compos 1984;5(3):202-207.

[7] Leblanc JL. Filled Polymers: Science and Industrial Applications. Boca Raton: CRC Press; 2010.

[8] Serafimow BL. Rheological properties of multicomponent mixtures based on polypropylene. Plaste Kautsch 1982;29(10):598-600.

[9] Comitov PG, Nicolova ZG, Simeonov IS, Naidenova KV, Siarova AD. Basic polypropylene compositions possessing an improved shock resistance. Eur Polym J 1984;20(4):405-407.

[10] Dao KC, Hatem RA. Properties of blends of rubber talc polypropylene. Plast Eng 1984;40(3):31-31.

[11] Dao KC, Hatem RA. Properties of blends of rubber/talc/polypropylene. SPE Antec 1984;84:198-204.

[12] Kolárík J, Lednický F. Structure of polypropylene/EPDM elastomer/calcium carbonate composites. In: Sedlácek B,

editor. Polymer Composites, Berlin: Walter de Gruyter; 1986, p. 537-544.

[13] Premphet K, Horanont P. Influence of stearic acid treatment of filler particles on the structure and properties of ternary-phase polypropylene composites. J Appl Polym Sci 1999;74(14):3445-3454.

[14] Hornsby PR, Premphet K. Influence of phase microstructure on the mechanical properties of ternary phase polypropylene composites. J Appl Polym Sci 1998;70(3):587-597.

[15] Pukánszky B, Kolárík J, Lednický F. Mechanical properties of three-component polypropylene composites. In: Sedlácek B, editor. Polymer Composites, Berlin: Walter de Gruyter; 1986, p. 553-560.

[16] Pukánszky B, Tüdős F, Kolárík J, Lednický F. Ternary composites of polypropylene, elastomer, and filler-analysis of phase-structure formation. Polym Compos 1990;11(2):98-104.

[17] Kelnar I. The Effect of PP and EPR grafted with acrylic-acid on the properties and phase-structure of polypropylene elastomer short glass-fiber composites. Angew Makromol Chem 1991;189:207-218.

[18] Chiang WY, Yang WD. Polypropylene composites. I. Studies of the effect of grafting of acrylic acid and silane

coupling agent on the performance of polypropylene mica composites. J Appl Polym Sci 1988;35(3):807-823.

[19] Chiang WY, Yang WD, Pukánszky B. Polypropylene composites. II. Structure-property relationships in 2-component and 3-component polypropylene composites. Polym Eng Sci 1992;32(10):641-648.

[20] Kolárík J, Lednický F, Jancár J, Pukánszky B. Phase-structure of ternary composites consisting of polypropylene/elastomer/filler: effect of functionalized components. Polym Commun 1990;31(5):201-204.

[21] Molnár S, Pukánszky B, Hammer CO, Maurer FHJ. Impact fracture study of multicomponent polypropylene composites. Polymer 2000;41(4):1529-1539.

[22] Bledzki AK, Sperber VE, Faruk O. Natural and wood fibre reinforcement. Shawbury: Rapra Technology; 2002.

[23] Bledzki AK, Gassan J. Composites reinforced with cellulose based fibres. Prog Polym Sci 1999;24(2):221-274.

[24] Bledzki AK, Faruk O, Huque M. Physico-mechanical studies of wood fiber reinforced composites. Polym-Plast Technol 2002;41(3):435-451.

[25] Bledzki AK, Mamun AA, Volk J. Physical, chemical and surface properties of wheat husk, rye husk and soft wood

and their polypropylene composites. Compos Part A-Appl S 2010;41(4):480-488.

[26] La Mantia FP, Morreale M. Green composites: A brief review. Compos Part A-Appl S 2011;42(6):579-588.

[27] Renner K, Móczó J, Pukánszky B. Deformation and failure of PP composites reinforced with lignocellulosic fibers: Effect of inherent strength of the particles. Compos Sci Technol 2009;69(10):1653-1659.

[28] Renner K, Kenyó C, Móczó J, Pukánszky B. Micromechanical deformation processes in PP/wood composites: Particle characteristics, adhesion, mechanisms. Compos Part A-Appl S 2010;41(11):1653-1661.

[29] Dányádi L, Renner K, Móczó J, Pukánszky B. Wood flour filled polypropylene composites: Interfacial adhesion and micromechanical deformations. Polym Eng Sci 2007;47(8):1246-1255.

[30] Nunez AJ, Sturm PC, Kenny JM, Aranguren MI, Marcovich NE, Reboredo MM. Mechanical characterization of polypropylene-wood flour composites. J Appl Polym Sci 2003;88(6):1420-1428.

[31] Li Q, Matuana LM. Effectiveness of maleated and acrylic acid-functionalized polyolefin coupling agents for HDPE-wood-flour composites. J Thermoplast Compos 2003;16(6):551-564.

[32] Kazayawoko M, Balatinecz JJ, Matuana LM. Surface modification and adhesion mechanisms in woodfiber-polypropylene composites. J Mater Sci 1999;34(24):6189-6199.

[33] Cantero G, Arbelaiz A, Mugika F, Valea A, Mondragon I. Mechanical behavior of wood/polypropylene composites: Effects of fibre treatments and ageing processes. J Reinf Plast Comp 2003;22(1):37-50.

[34] Lu JZ, Wu QL, Negulescu, II. Wood-fiber/high-density-polyethylene composites: Coupling agent performance. J Appl Polym Sci 2005;96(1):93-102.

[35] Clemons C. Elastomer modified polypropylene-polyethylene blends as matrices for wood flour-plastic composites. Compos Part A-Appl S 2010;41(11):1559-1569.

[36] Oksman K. Improved interaction between wood and synthetic polymers in wood/polymer composites. Wood Sci Technol 1996;30(3):197-205.

[37] Oksman K, Clemons C. Mechanical properties and morphology of impact modified polypropylene-wood flour composites. J Appl Polym Sci 1998;67(9):1503-1513.

[38] Keledi G, Sudár A, Burgstaller C, Renner K, Móczó J, Pukánszky B. Tensile and impact properties of three-component PP/wood/elastomer composites. Express Polym Lett 2012;6(3):224-236.

[39] Dányádi L, Janecska T, Szabó Z, Nagy G, Móczó J, Pukánszky B. Wood flour filled PP composites: Compatibilization and adhesion. Compos Sci Technol 2007;67(13):2838-2846.

[40] Thio YS, Argon AS, Cohen RE, Weinberg M. Toughening of isotactic polypropylene with $CaCO_3$ particles. Polymer 2002;43(13):3661-3674.

[41] Pukánszky B, Maurer FHJ. Composition dependence of the fracture toughness of heterogeneous polymer systems. Polymer 1995;36(8):1617-1625.

[42] Wang K, Wu J, Ye L, Zeng H. Mechanical properties and toughening mechanisms of polypropylene/barium sulfate composites. Compos Part A-Appl S 2003;34(12):1199-1205.

[43] Rong MZ, Zhang MQ, Zheng YX, Zeng HM, Walter R, Friedrich K. Structure–property relationships of irradiation grafted nano-inorganic particle filled polypropylene composites. Polymer 2001;42(1):167-183.

[44] Selvin TP, Kuruvilla J, Sabu T. Mechanical properties of titanium dioxide-filled polystyrene microcomposites. Mater Lett 2004;58(3–4):281-289.

[45] Wilbrink MWL, Argon AS, Cohen RE, Weinberg M. Toughenability of Nylon-6 with $CaCO_3$ filler particles: new findings and general principles. Polymer 2001;42(26):10155-10180.

[46] Zhang QX, Yu ZZ, Xie XL, Mai YW. Crystallization and impact energy of polypropylene/$CaCO_3$ nanocomposites with nonionic modifier. Polymer 2004;45(17):5985-5994.

[47] Singleton ACN, Baillie CA, Beaumont PWR, Peijs T. On the mechanical properties, deformation and fracture of a natural fibre/recycled polymer composite. Compos Part B-Eng 2003;34(6):519-526.

[48] Dányádi L, Renner K, Szabó Z, Nagy G, Móczó J, Pukánszky B. Wood flour filled PP composites: adhesion, deformation, failure. Polym Advan Technol 2006;17(11-12):967-974.

[49] Pukánszky B. Effect of interfacial interactions on the deformation and failure properties of PP/$CaCO_3$ composites. New Polym Mat 1992;3:205-217.

[50] Seymour RB. Origin and early development of rubber-toughened plastics. Adv Chem Ser. 1989(222):3-13.

[51] Bucknall CB. Toughened plastics. London: Applied Science Publishers; 1977.

[52] Pearson RA, Sue HJ, Yee AF. Toughening of plastics. Washington: American Chemical Society; 2000.

[53] Riew CK, Kinloch AJ. Toughened plastics I. Washington: American Chemical Society; 1993.

Table 1 Particle characteristics of the wood fibers used in the experiments

Fiber	Abbreviation	D[4,3][a] (μm)	Length[b] (μm)	Diameter[b] (μm)	Aspect ratio[b]
Arbocel UFC M8	W10	12.0	14.2 ± 8.3	4.8 ± 2.8	3.19 ± 1.63
Arbocel CW 630 PU	W40	42.2	45.8 ± 28.2	17.6± 10.5	2.83 ± 1.48
Filtracel EFC 1000	W160	162.9	137.4 ± 136.1	35.2 ± 33.2	4.16 ± 2.6

a) volume average particle size
b) average values determined from scanning electron micrographs

Captions

Fig. 1 Impact resistance of hPP/wood composites plotted as a function of wood content. Effect of particle size and interfacial adhesion. Notched, 23 °C. Symbols: (△) W10, (□) W40, (○) W160, empty: no coupling, full: MAPP.

Fig. 2 Instrumented impact traces of a series of hPP/wood composites. Notched Charpy impact, 23 °C, W160, MAPP.

Fig. 3 Effect of compositional variables on the un-notched Charpy impact resistance of hPP/wood composites. Symbols: (△) W10, (□) W40, (○) W160; no coupling.

Fig. 4 Force vs. time traces recorded in the instrumented impact testing of hPP/wood composites. Un-notched Charpy impact, 23 °C, W160, no coupling.

Fig. 5 SEM micrographs taken from the fracture surface created during the impact testing of hPP/wood composites. a) 10 wt% W160, b) 10wt% W10; MAPP.

Fig. 6 Notched Charpy impact resistance of PP/elastomer blends plotted against their elastomer content, 23 °C.

Fig. 7 Instrumented impact traces of PP/elastomer blends; notched, 23 °C.

Fig. 8 Composition dependence of the Young's modulus of three-component hybrid composites indicating the extent of embedding. Symbols: (△) W10, (□) W40, (○)

W160, empty: MAEPDM, full: MAPP.

Fig. 9 Independence of notched Charpy impact resistance of structure; dominating effect of wood content. Symbols: (△) W10, (□) W40, (○) W160, empty: MAEPDM, full: MAPP, 23 °C.

Fig. 10 Instrumented impact traces of PP/elastomer/wood hybrid composites. Notched, 23 °C, 43 wt% elastomer, MAPP.

Fig. 11 SEM micrograph recorded on the fracture surface created in impact testing of hybrid ePP composites; 33 wt%; a) 30 wt% W160, MAEPDM, b) 10 wt% W10, MAEPDM, c) 30 wt% W10, MAPP, cavitation.

Fig. 12 Close correlation between the notched Charpy impact resistance and the stiffness of the composites investigated in this study. Symbols: (△?;7) W10, (□)%!) W40, (○354012,) W160, (;%0) no coupling,(△□○32) MAEPDM, (7!51,) **MAPP?**, (?;,)%,40) homopolymer, (21) 20 wt% elastomer, (△7□!○,) 33 wt% elastomer, (35) 43 wt% elastomer.

Fig. 13 Stress vs. deformation and volume strain vs. deformation correlations recorded on hPP and ePP, respectively. ——— hPP, ------ ePP.

Fig. 14 Effect of the method of incorporation on the impact resistance of PP/elastomer blends. Symbols: (●)

reactor blend, (■) physical, melt blend.

Fig. 15 Dominating deformation mechanism in PP/elastomer blends. a) melt blend, 20 wt% elastomer, b) reactor blend, 33 wt% elastomer.

Figures

Sudár, Fig. 1

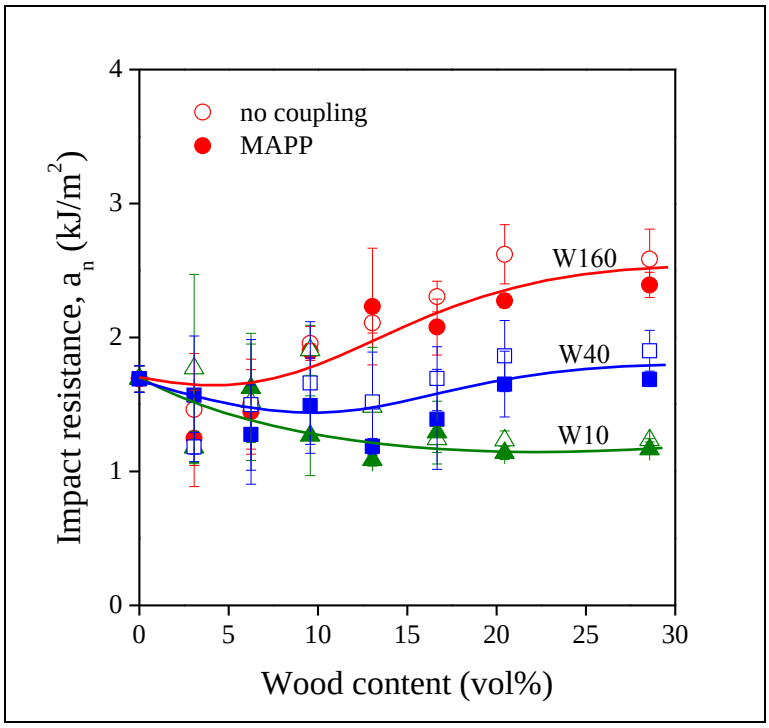

Sudár, Fig. 2

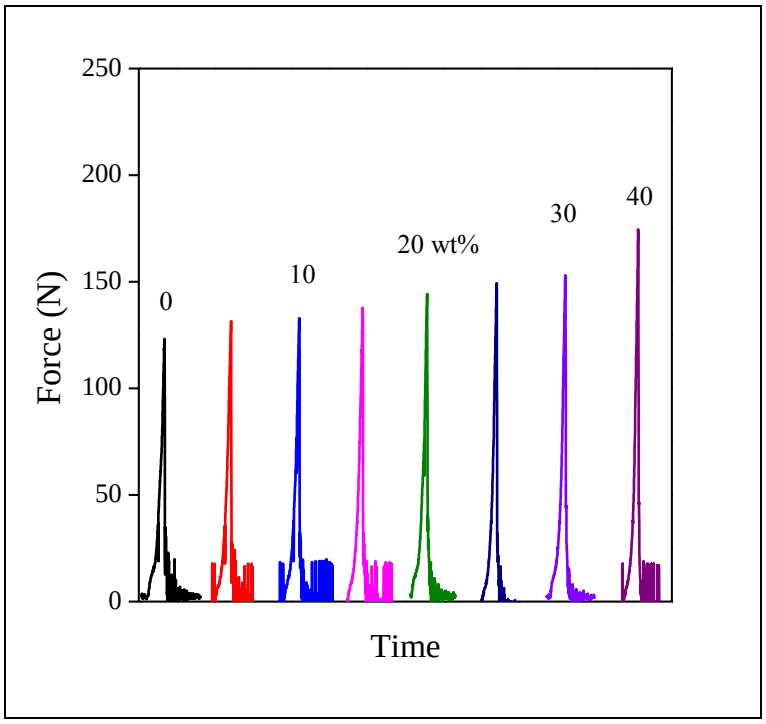

Sudár, Fig. 3

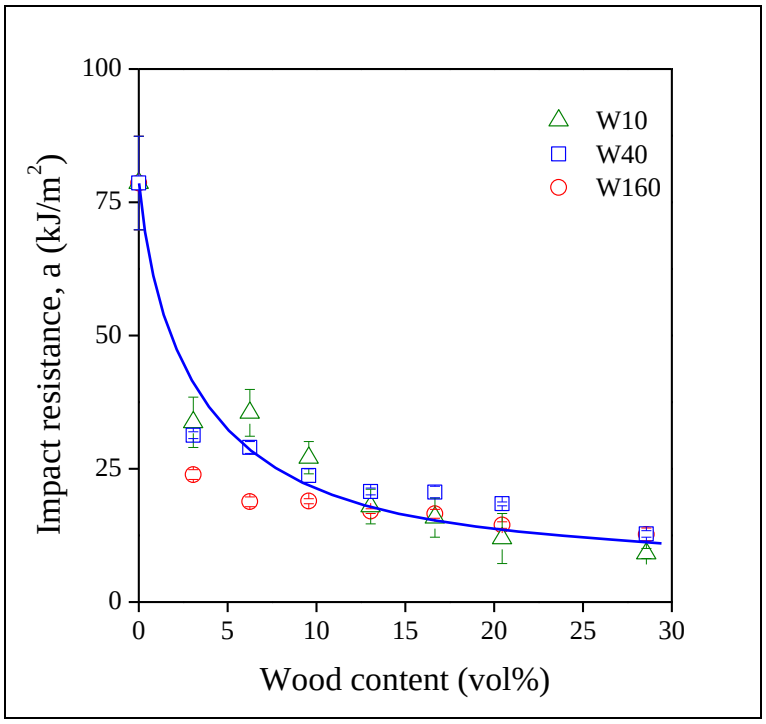

Sudár, Fig. 4

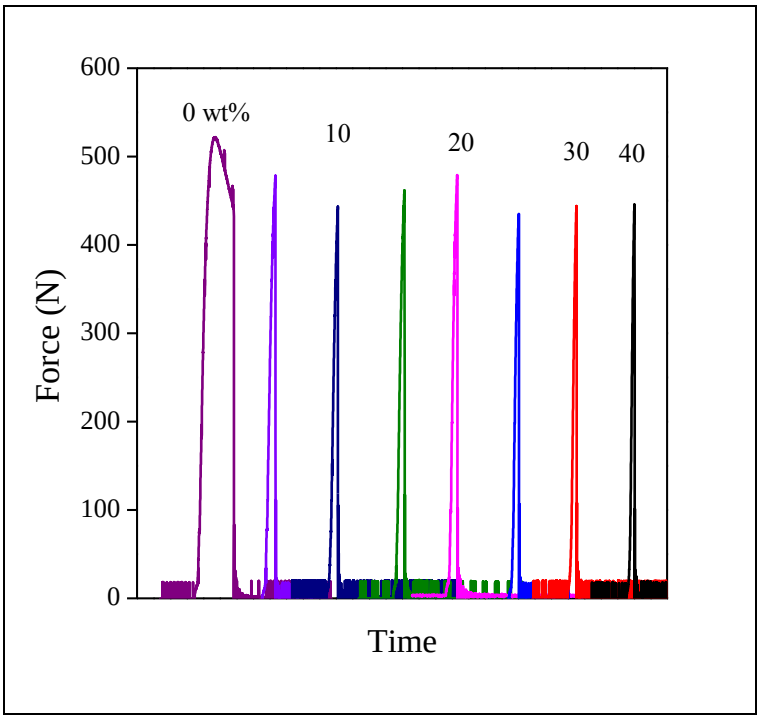
600
500
400
300
200
100
0
Force (N)
0 wt%
10
20
30
40
Time

Sudár, Fig. 5

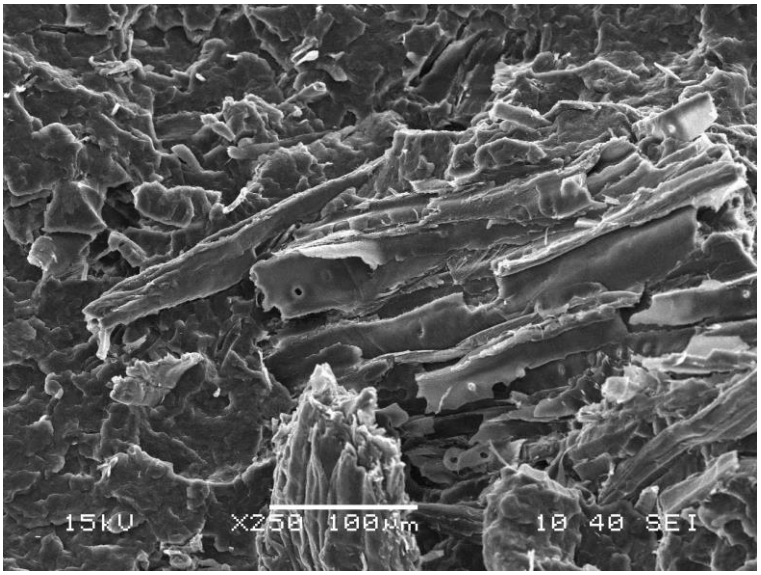
15kV
X250 100µm
10 40 SEI

a)

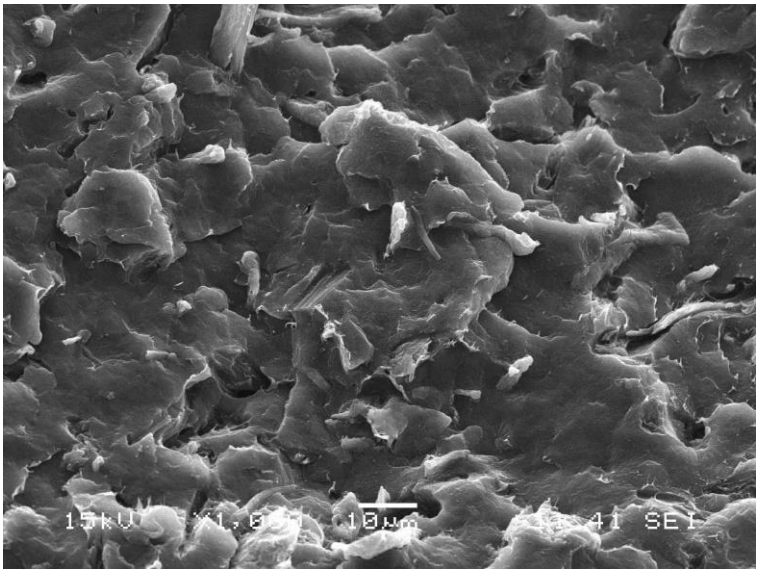
15kV X1,000 10μm 41 SEI

b)

Sudár, Fig. 6

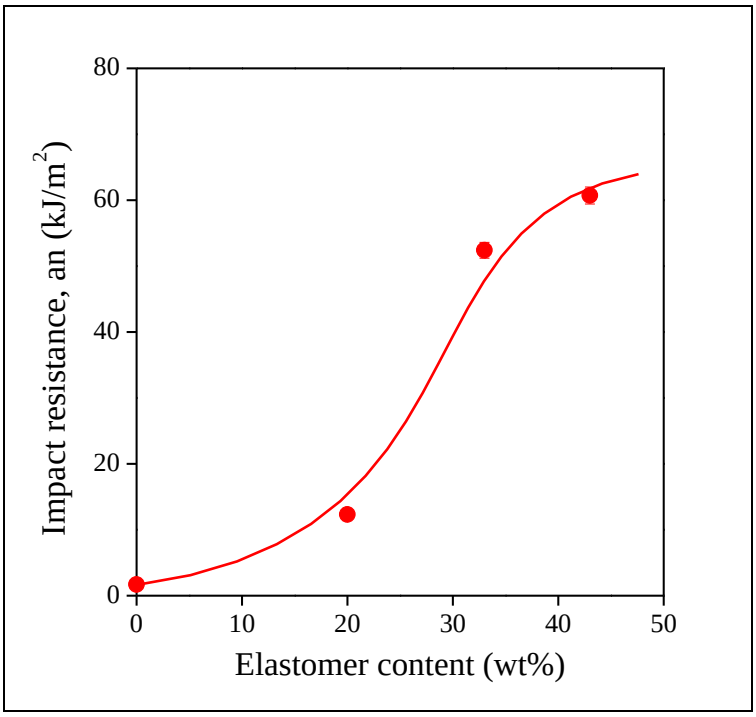
Impact resistance, an (kJ/m2)
Elastomer content (wt%)
0
20
40
60
80
0
10
20
30
40
50

Sudár, Fig. 7

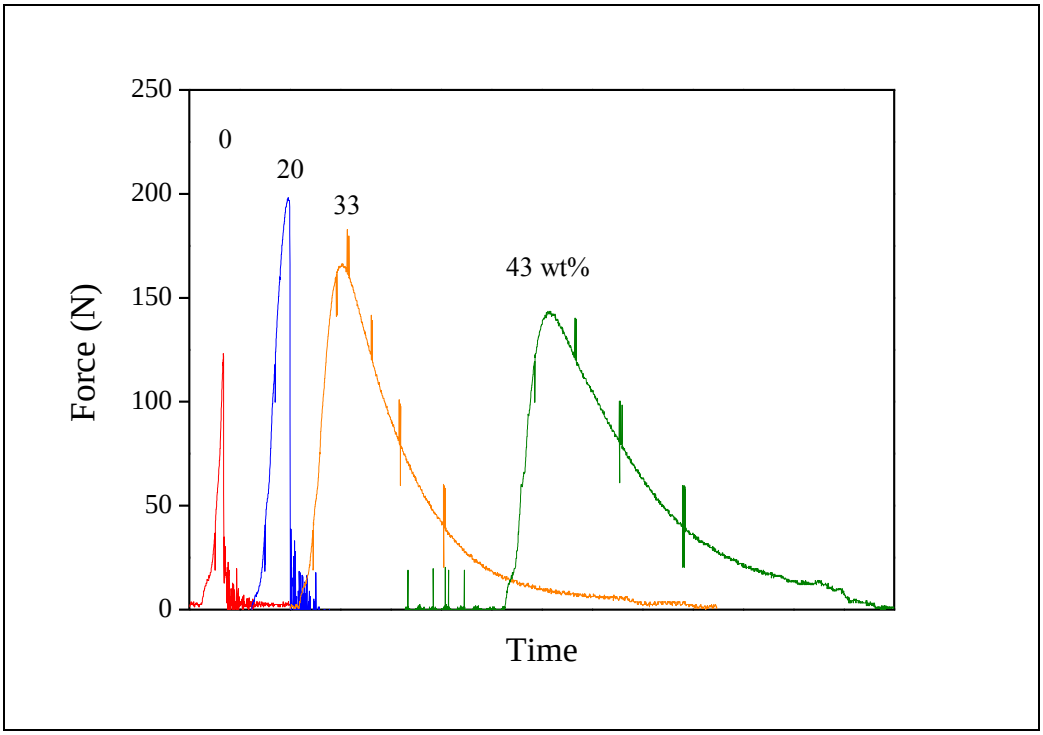

Sudár, Fig. 8

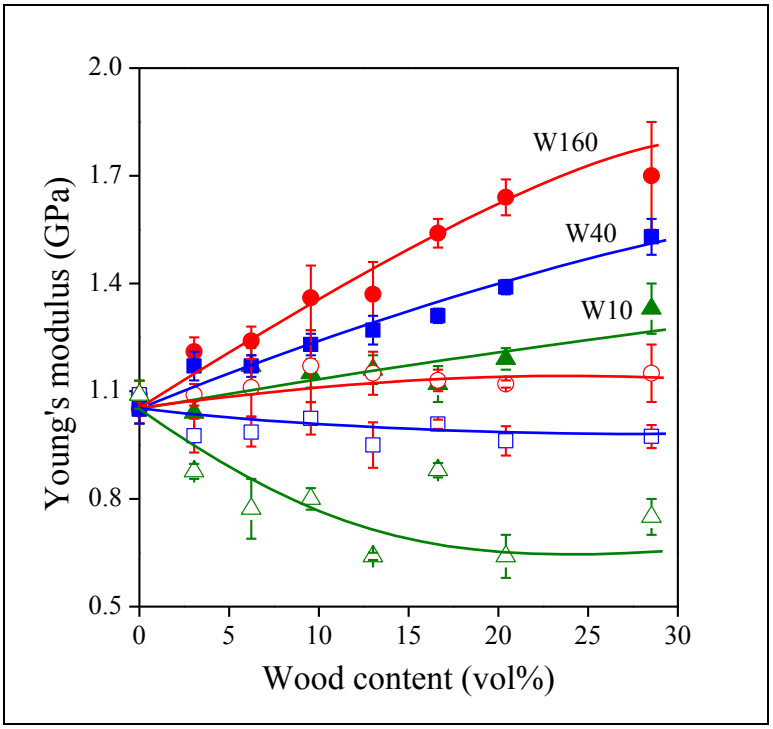

Sudár, Fig. 9

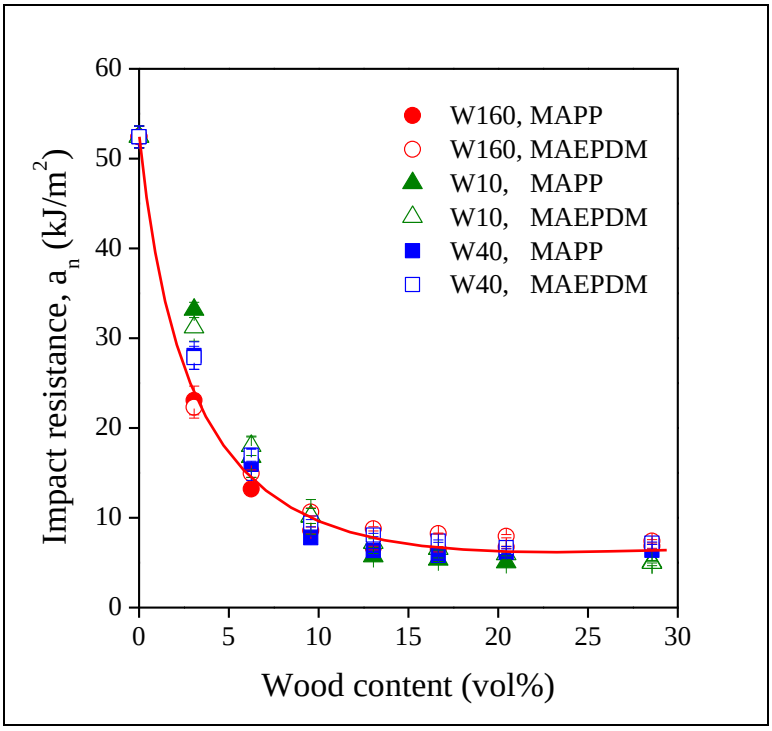

Sudár, Fig. 10

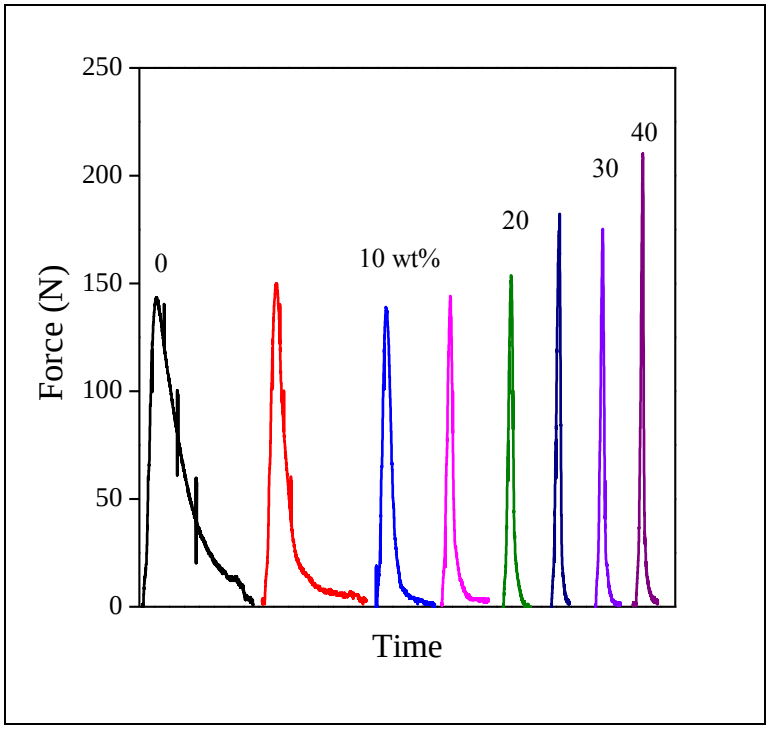

Sudár, Fig. 11

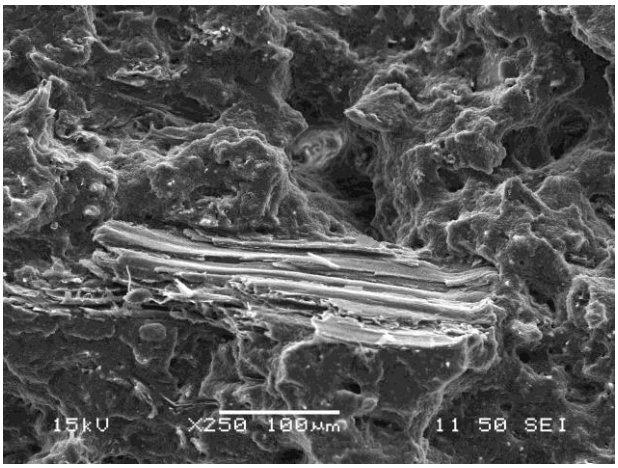

a)

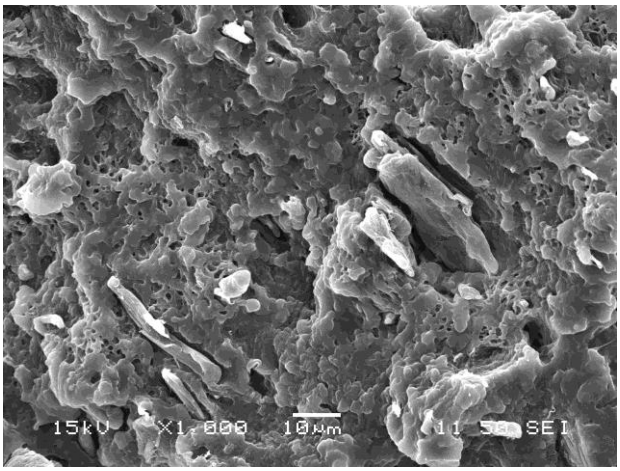

b)

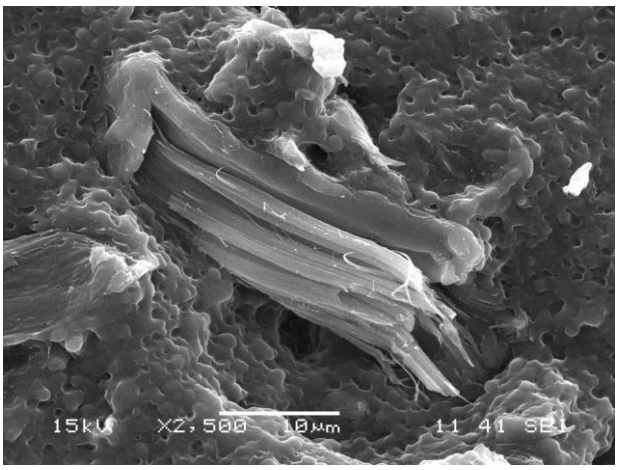

c)

Sudár, Fig. 12

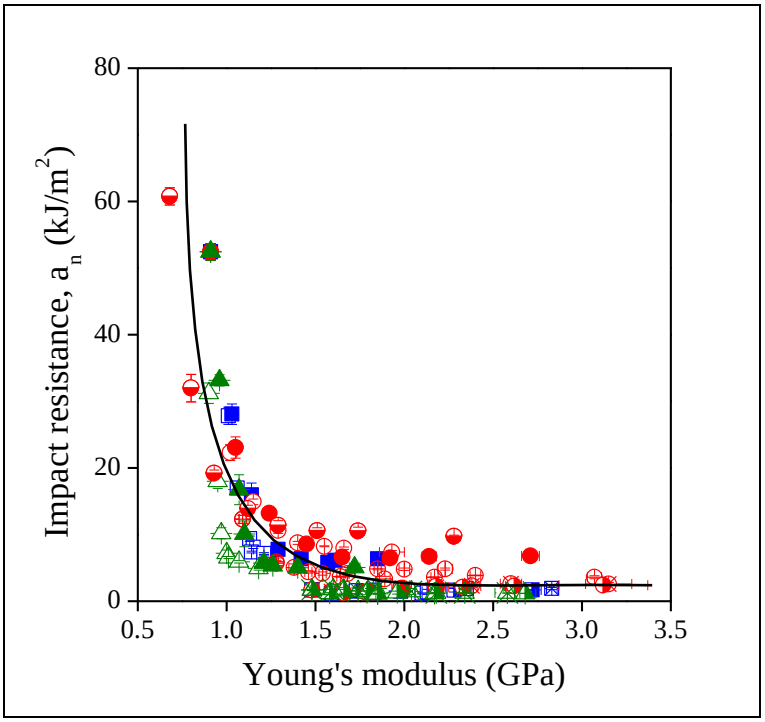

Sudár, Fig. 13

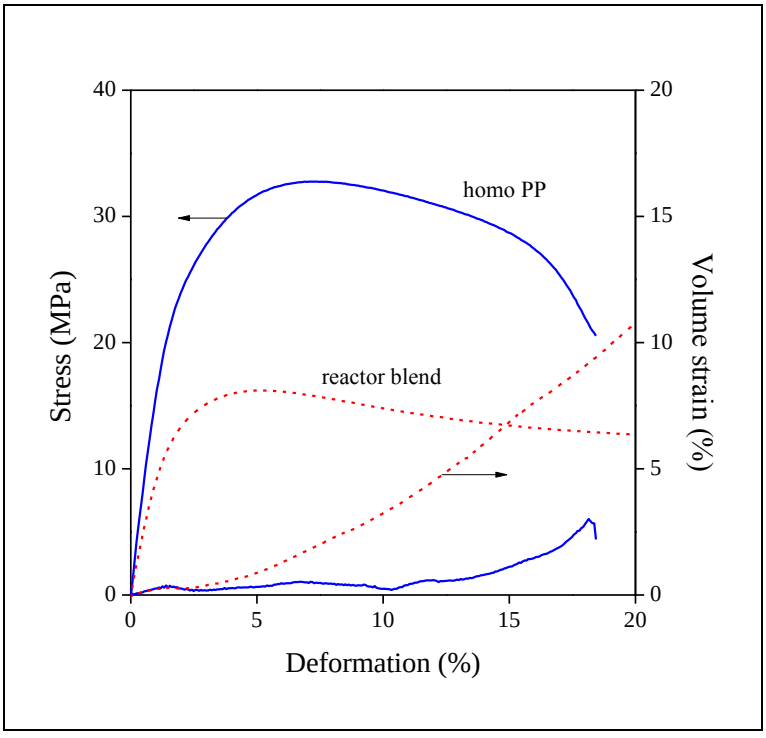

Sudár, Fig. 14

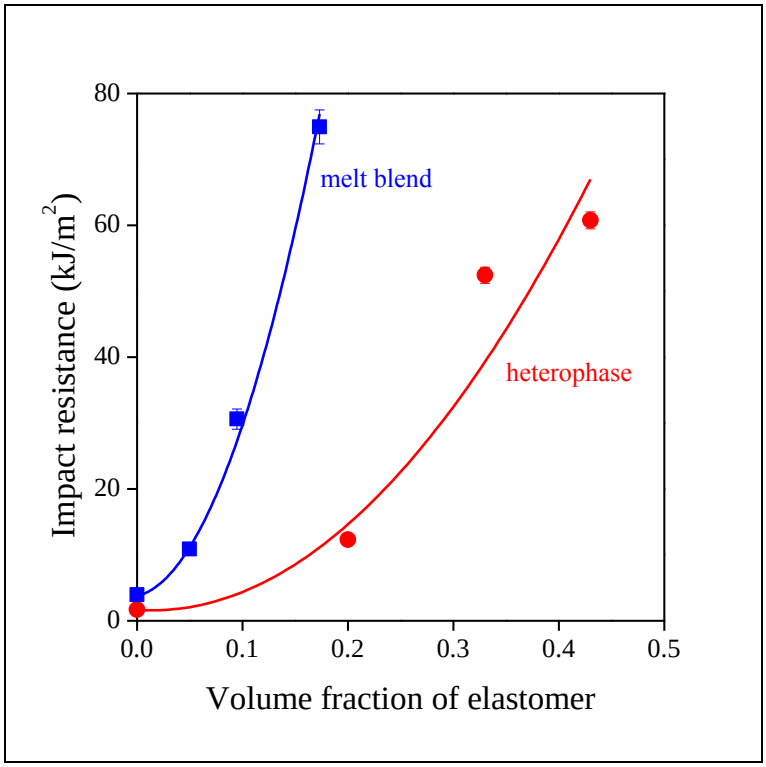
80
60
40
20
0
0.0
0.1
0.2
0.3
0.4
0.5
Impact resistance (kJ/m2)
Volume fraction of elastomer
melt blend
heterophase

Sudár, Fig. 15

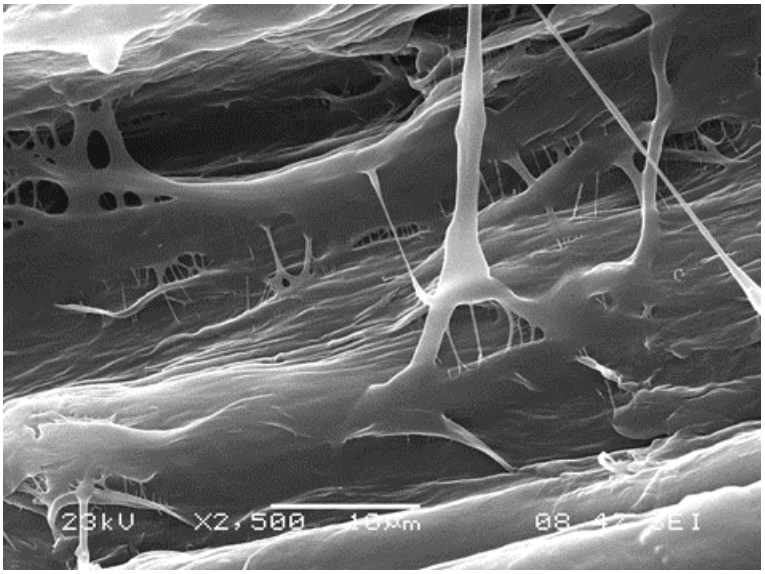

a)

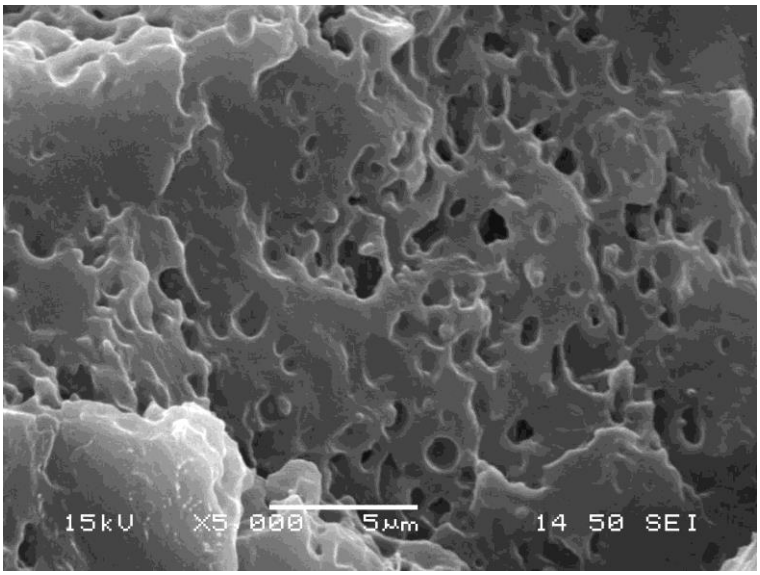

b)